FABRICATION AND CHARACTERIZATION OF NOVEL ULTRA-SENSITIVE GLUTAMATE AND GABA OPTICAL FIBER BIOSENSOR PROBES

By

JULIA MARIE CORDEK

A DISSERTATION PRESENTED TO THE GRADUATE SCHOOL
OF THE UNIVERSITY OF FLORIDA IN PARTIAL FULFILLMENT
OF THE REQUIREMENTS FOR THE DEGREE OF
MASTER OF SCIENCE

UNIVERSITY OF FLORIDA

A

1998

This thesis is dedicated to the memory of my father, David Cordek. His belief in me shows in everything I do.

ACKNOWLEDGMENTS

Graduate school has proven to be one of the most challenging endeavors of my professional life. It has altered my view on many aspects of life, aside from my perspective on science. I was able to celebrate this experience, due to the constant reinforcement from my wonderful family and dear friends.

I would like to thank Dr. Weihong Tan for his generous support and leadership. I was very fortunate to be able to work in such a new and exciting field of chemistry. I owe great appreciation to the entire Tan Research Group, particularly to Valerie Gallion. Her strength and example paved the way for my accomplishment.

I am especially thankful to Jennifer Tonzello for her gracious counsel, continual support and all around warm-hearted nature.

I am profoundly indebted to Dr. David Rusak. Without his guidance, support and esteem, I would have gone to fight fires without a drop of water.

TABLE OF CONTENTS

Page Number

ACKNOWLEDGMENTS iii

LIST OF FIGURES vi

ABSTRACT viii

CHAPTER

1 INTRODUCTION 1
  1.1 Historical Survey 7
  1.2 Scope of Research 10
2 GLUTAMATE AND GABA 12
  2.1 Role As Neurotransmitters 12
  2.2 Current Methods of Detection 14
  2.3 Enzyme-based Fluorescent Optical Fiber Probe 15
  2.4 *In-vivo* Issues of Glutamate and GABA Detection 17
  2.5 Summary: Why use Micrometer Fiber Probes? 18
3 EXPERIMENTAL CONSIDERATIONS 20
  3.1 Instrumentation 20
    3.1.1 Experimental Set-Up 20
    3.1.2 Microscopic Probe Imaging. 21
  3.2 Reagents and Materials 22
  3.3 Procedures 23
    3.3.1 Pulling and Etching Optical Fiber Tips 23
    3.3.2 Optical Fiber Probe Surface Modification 24
    3.3.3 Enzyme Immobilization - GDH. 25
    3.3.4 Enzyme Immobilization - GABAse. 26
  3.4 Sensor Response Analysis 27
    3.4.1 Measurements in Pre-formed Membrane Wells 27
4 FABRICATION AND CHARACTERIZATION OF THE GLUTAMATE SENSOR 29
  4.1 Results and Discussion 29
    4.1.1 Direct Covalent Immobilization of GDH on Optical Fiber Surface. 29

4.1.2 Effect of Immobilization Time on GDH Probe's Activity.............30
4.1.3 NAD$^+$ and Glutamate Affect on GDH Immobilization..................32
4.1.4 NAD$^+$ Affect on Glutamate Sensor Performance............................32
4.1.5 GDH Probe for Sensitive Glutamate Detection. 32
4.1.6 Glutamate Sensor Stability and Selectivity. 35
4.1.7 Glutamate Sensor Response Time..38
4.1.8 Submicrometer Glutamate Sensors. 38
4.2 Conclusions 40
FABRICATION AND CHARACTERIZATION OF THE GABA SENSOR 42
5.1 Results and Discussion...42
5.1.1 Fluorescent Response of GABA 42
5.1.2 Influence of pH...48
5.1.3 Compared Performance of Sensor Stability. 50
5.1.4 Sensitivity and Detection Limit of the Fiber Optic Sensor. 50
5.2 Conclusions 55
CURRENT AND FUTURE APPLICATIONS...56
6.1 Immobilization Techniques..56
6.2 Nanofabrication of Probes...57
6.3 Multi-Functional Senors...58
6.4 Optical Set-Up..60
6.5 Synopsis 62
LIST OF REFERENCES 63
BIOGRAPHICAL SKETCH...66

LIST OF FIGURES

Figure 1.1 Conceptual diagram of NFO. 2

Figure 1.2 Schematic of light rays obeying Snell's Law. 4

Figure 1.3 Schemetic of three forms of optical fiber waveguides. 'n' is the refractive index of the different materials..5

Figure 3.1 Schematic diagram of the optical set-up for enzyme probe measurements....21

Figure 3.2 Detection of primary amines on the fiber surface before conjugation. 25

Figure 3.3 Immobilization of glutamate dehydrogenase on a fiber optic surface............26

Figure 3.4 View through the objective lens after injection of the capillary with substrate. 28

Figure 4.1 Effect of immobilization time on the sensor response. NAD^+ and glutamate concentrations were 1mM and 4mM, respectively..31

Figure 4.2 Effect of NAD^+ concentration on the glutamate sensor activity.....................33

Figure 4.3 Glutamate calibration plot using a GDH probe with NAD^+ concentration at 1mM. 34

Figure 4.4 Response to 1mM glutamate and 4mM NAD^+ as a function of sensor age. ..36

Figure 4.5 Selectivity of GDH probe for glutamate over physiological interferences. ...37

Figure 4.6 Response of two GDH probes are shorter than 50 ms. NAD^+ and glutamate concentrations were 1mM and 1mM, respectively..39

Figure 4.7 Glutamate calibration plot using a 5μm etched GDH probe. NAD^+ was 1mM. 40

Figure 4.8 Glutamate monitoring in a 5 μm polycarbonate membrane hole by a submicrometer GDH probe. 41

Figure 5.1 Immobilization of the two enzymes of GABAse on a fiber optic surface......44

Figure 5.2 (a) 1. - Free GABAse in solution in the presence of 1mM GABA, α-KG and $NADP^+$. 2. - Free GABAse in the same solution as 1, but without GABA. (b) 1. - Immobilized GABAse in the presence of 1mM GABA, α-KG and $NADP^+$. 2. - Immobilized GABAse in the same solution as 1, but without GABA. 46

Figure 5.3 Effect of immobilization time on the sensor response. $NADP^+$, α-KG and GABA were 1 mM. 47

Figure 5.4 Influence of pH on the GABA fiber sensor. $NADP^+$ was 1 mM and α-KG and GABA were 100 μM. 48

Figure 5.5 Minimum recovery time needed to eliminate fluorescence and begin new run. $NADP^+$, α-KG and GABA were 400 μM. 49

Figure 5.6 Effect of $NADP^+$concentration on the GABA sensor activity........................ 51

Figure 5.7 Effect of α-KG concentration on the GABA sensor activity. 52

Figure 5.8 GABA calibration plot using a GABAse probe with $NADP^+$ and α-KG at 1 mM. 53

Figure 5.9 Linear range of detection for GABA sensor. $NADP^+$ and α-KG are at 1 mM. 54

Figure 6.1 CCD image of preliminary cellular applications of a micrometer sized glutamate fiber sensor.. 59

Figure 6.2 Schematic drawing of simultaneous determination of extracellular glutamate and intracellular calcium in ischemic neuronal damage... 61

Abstract of Thesis Presented to the Graduate School
of the University of Florida in Partial Fulfillment of the
Requirements for the Degree of Master of Science

FABRICATION AND CHARACTERIZATION OF NOVEL ULTRA-SENSITIVE GLUTAMATE AND GABA OPTICAL FIBER BIOSENSOR PROBES

By

Julia Cordek

December 1998

Chairman: Weihong Tan
Major Department: Department of Chemistry

Ultrasensitive glutamate and GABA monitoring is crucial to the analysis and understanding of neuronal transmission and nervous system disease (stroke and/or epilepsy). The general method in optical fiber sensing is discussed in this work. With the creation of submicrometer fiber optic biosensors, future *in vivo* fluorescence analysis will be accomplished utilizing Near Field Optics (NFO). We have developed glutamate and GABA biosensors with exceptional sensitivity, advanced response times and micrometer to submicrometer sizes. Glutamate dehydrogenase (GDH) and GABAse [a combination of two enzymes, γ-aminobutylate ketoglutarate aminotransferase (GABA-T) and succinic semialdehyde dehydrogenase (SSDH)] have been applied as working enzyme systems immobilized onto optical fiber probe surfaces through newly developed covalent binding mechanisms. None of the direct or indirect physical confinement methods, such as mechanical confinement, gel trapping or membrane immobilization, have been used in the sensors' preparation. An optical fiber surface is initially activated by silanization. We then affix carboxyl functional groups to the optical fiber surface by employing a bifunctional cross-linking agent, glutaraldehyde. The amino acids of the enzyme molecules readily attach to the free carboxyl groups on the fiber surface. Optimal immobilization of the enzymes occurred between 19 and 23 hours in enzyme solution. The enzymes on the fiber surface have shown high enzymatic activity. The sensors are able to detect each enzyme's specific substrate, glutamate or GABA, by monitoring the fluorescence of reduced nicotinamide adenine dinucleotide (NADH) or nicotinamide adenine dinucleotide phosophate (NADPH), a product of the enzymatic reactions. The concentration detection limit of the glutamate sensor is 0.2 μM, and the absolute mass detection limit is 3.5 attomoles. The linear range detection limit for the GABA sensor is 0.92 μM. The response time of the glutamate sensor is fast due to the direct immobilization of the GDH molecules on the probe and the high activity of the enzyme. GABAse has an inherently lower activity, and therefore its response times are slightly lower. The sensors are stable when stored over 3 days and extremely selective. Submicrometer glutamate sensors, producing very noninvasive bioanalytical tools, have been tested in microliter polycarbonate membrane holes and on cellular level neurotransmitter release. Future GDH probes will be applied to the study of cellular level neurophysiological response in glutamate release monitoring experiments. The results of these experiments will pave the way for the study of cellular GABA release, and subsequently real-time, dual neurotransmitter release monitoring.

CHAPTER 1
INTRODUCTION

Traditional optical techniques are based on focusing elements such as a lens. The sample is usually situated at a relatively large distance from the light source. In such *far-field optics*, the standard rules of interference and diffraction lead to the Abbè diffraction limit (1873) [1] on the resolution of optical microscopes. This limit is approximately $\lambda/2$, where λ is the wavelength. Technology in the physical and biological sciences has created the demand for better resolution. Therefore, the realization of better resolution with sub-wavelength light sources has led to the concept of near-field optics (NFO). NFO has made it possible to circumvent the optical diffraction limit through the use of a small light source that effectively focuses photons through an aperture that can be as small as $\lambda/50$. Samples are then positioned very close to the sub-wavelength light source, or in the near-field. This theory is demonstrated in Figure 1.1. To form the NFO probe, light is directed to an opaque screen containing a small aperture. The aperture acts as a scanning probe to generate an image of a sample in the near-field region. Therefore, this type of microscopy has become known as near-field scanning optical microscopy (NSOM).

Near-field optics, such as NSOM, has been utilized for a variety of applications. There are many other near-field microscopy techniques that have been developed such as Scanning Tunneling Microscopy (STM), thermal microscopy, Atomic Force Microscopy

(AFM), and the ion-probe. Each procedure uses a different type of probe mechanism to create contrast, and hence collect information on the specimen being examined.

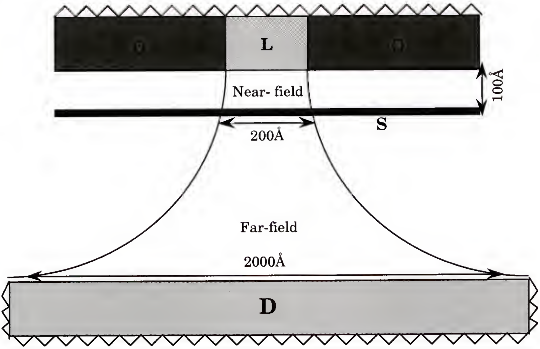

L: Active or passive light source;
O: Opaque Material;
S: Sample (support not shown);
D: Far Field Detection System(e.g. lens).

Figure 1.1 Conceptual diagram of NFO.

The uniqueness of NSOM is specifically the probe. The probes can be divided into two classes, active or passive light sources. Passive light probes are dependent on apertures and near-field scattering mechanisms. Active light probes are dependent on luminescence effects, or absorption and fluorescence mechanisms. An ideal light source for these probes, must be small, intense, durable and spatially controllable. In this thesis, the significant semi-active light source, which meets all of the requirements, is the optical fiber probe.

Optical fibers are, in basic terms, "wires for light" or waveguides. The optical energy will be transported through a transparent material only if the size of the waveguide transverse to the direction of incident light is of the order of the size of the wavelength of light or more. Light propagated on a boundary between two transparent media with differing refractive indices (n) obeys Snell's law, as shown in Figure 1.2.

$$n_1 \sin\theta_1 = n_2 \sin\theta_2 \quad (1.1)$$

If the light is incident to the interface at an angle greater than the angle of refraction of 90°, then this angle is known as the critical angle θ_c, defined as:

$$\sin\theta_c = n_2/n_1 \quad (1.2)$$

When this critical angle occurs, then there are no refracted rays and only total internal reflected (TIR) light rays. The term total refers to the fact that there will be no decrease of the light as it propagates down the waveguide. This is in contrast to a mirror that may lose 4% of reflection [2]. A typical optical fiber consists of an inner core, made of glass or plastic, with a refractive index, n_1, and two concentric outer coatings. The first outer coating is called the cladding and must have a refractive index, n_2, less than n_1. Only those rays that are internally reflected can be propagated along the fiber. Light outside this critical angle is not trapped and is passed into the cladding where it is dissipated as scattered light. The most external layer is termed the jacket, or buffer, and forms a protective and durable coating.

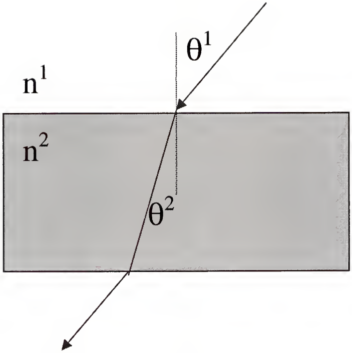

Figure 1.2 Schematic of light rays obeying Snell's Law.

Optical fibers can be classified into three forms that all behave as waveguides. The refractive index profiles and the number of modes the fiber will support hold the most informative means of organization. A mode is just a path that a light beam may travel through the fiber. Figure 1.3 demonstrates the three forms.

Multi-mode step index fibers have the advantage that they are inexpensive, large numerical aperture cores are available (50 – 1,000 μm), and they are easy to couple to an original light source. The step index means that the fiber only has two refractive indices that form a step from the core to the cladding. The disadvantage is that, in a pulsing mode, there is large dispersion of different wavelengths of light.

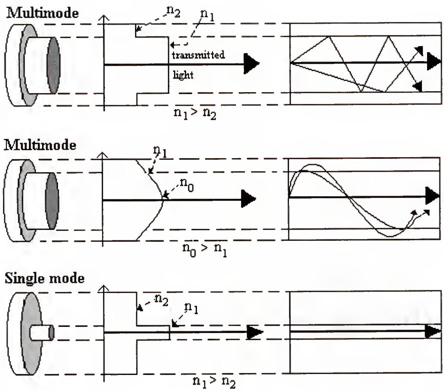

Figure 1.3 Schemetic of three forms of optical fiber waveguides. ‘n’ is the refractive index of the different materials.

The single mode fibers have the advantage that there is little dispersion with wavelength and that small numerical apertures are available, with core diameters ranging from 2 – 10 μm. They support only one guided mode at their operating wavelength. The disadvantages are that they are fairly difficult to work with and they require special connectors to couple them to the laser light source. The multi-mode graded index fibers have properties in between the two types mentioned above. This fiber has an inner core diameter of 50 – 100 μm with a refractive index that decreases in an outward radial pattern. This was developed to reduce the modal dispersion that can occur in the multi-mode step index fiber.

A key requirement for fabrication of an optical fiber sensor device is a connector or coupler, so that the laser beam is positioned onto the core efficiently. Ideally, when light intensities are being measured, the loss in coupling should be negligible. As stated earlier, multimode fibers are somewhat easier to couple due to their larger cores. Single mode fibers are more difficult and require special couplers with submicron positioning resolution. Ordinary lenses can be used to focus the laser light into an optical fiber. The characteristics of the focused beam must match the fiber parameters for good coupling efficiency. General guidelines are as follows:

a. The focused spot should be comparable to the core size.
b. The incident cone angle should not exceed the arcsine of the numerical aperture (NA) of the fiber.
c. For single mode fibers, one has to match the incident field distribution to the mode of the fiber.

Recent development in optically based chemical and biological sensor technology has led to a new generation of miniature fiber optic biosensors [1]. A wide range of assays have been developed into sensors that have a common base of an immobilized component that changes its optical properties upon affinity to an analyte. As a result of developments in the communications industry, single optical fibers are available with excellent transmission characteristics and an assembly of couplers, light sources, filters, and light detectors. Extremely pure materials have been used in the fabrication of fibers to reduce attenuation of the signal and the costs of fibers are continually decreasing. One can now see the relevance and great benefits of using the special characteristics of optical fibers with near-field optics for creation and application of biosensors.

1.1 Historical Survey

Fiber optic technology is a fairly recent tool arising in chemistry applications. One main concern involved with fiber optic technology is the availability of a fiber small enough to probe a biochemical medium with sub-micrometer resolution and non-invasive properties. The fabrication of sub-micrometer optical fiber probe tips was accomplished in 1991 by Betzig et al. [3]. This advancement broke the diffraction barrier of traditional microscope's spatial resolution. The sample was brought into close proximity to the light source, thus allowing the scanning of a spot of light smaller then the optical wavelength such that far-field diffraction effects could not occur. Elimination of the diffraction limit transpired and limitation based on probe size began. The race to single molecule sensitivity started because researchers now had a tool through which light is confined to pass through a small aperture (100nm). High photon flux could be delivered to the end of the probe with less power, therefore enabling near background free detection.

The next problem dealt with isolating the analysis procedure nearer to the fiber tips surface, significantly reducing analyzing volume and accomplishing ultra-sensitivity. There existed a need for confining the detection chemistry to the fiber surface. For example, sensing methodology which involves the use of various mechanical methods of placing the chemical reagent on the fiber surface are difficult to achieve; such sensors usually have slow response times. These problems were overcome by covalent immobilization of reagents on the distal end of an optical fiber by photopolymerization in

1986 [4]. Kopelman et al. enhanced this technology in 1992 when the first sub-micron chemical sensor combining nano-scaled fabricated tips with polymerization was reported [5]. This pH sensor was produced by drawing single-mode and multimode optical fibers into sub-micron fiber tips using a micropipette puller, which was originally developed for the manufacture of micro-electrodes. The cone surface of the fiber tip was subsequently overlaid with aluminum leaving the end surface as a transmissive aperture. Spatially controlled photopolymerization was used to form a polymer-fluorescent pH indicator on the fiber tip. Using an inverted microscope, it was possible to maneuver the sensor tips into microwells containing varying pH buffers and subsequently record the fluorescence spectra. It was reported that these sensors had very quick response times, in the range from 100 to 500 ms, implying that the confinement of the reaction was at the tip surface. The samples were scanned at a distance much smaller than the wavelength of light to obtain high resolution optical information that was not diffraction limited.

This type of sensor is in the class of what are termed extrinsic fiber optic chemical sensors. This type of chemical sensor acts to guide the examining light to the immobilized reagent, which in turn changes its optical properties upon interaction with the analyte. Extrinsic chemical sensors are based on indicator-mediated sensing, which is convenient when analytes do not have useful intrinsic absorption or fluorescence (i.e.: oxygen and pH) and therefore can not be sensed directly. Fiber sensing technologies have been developed in which the analytical information is dependent on indicator chemistry, which is typically an active layer of an immobilized reagent on the waveguide surface. Such sensors have spectral properties which reflect the analyte concentration.

Tan, Shi and Kopelman made huge contributions to the advancement of miniaturized fiber optic sensor technology [5]. These sensors used photopolymerization techniques, in which the sensing component was trapped within the polymer gel which is covalently attached to the polymer surface. The oxygen sensor, which was the first capable of measuring oxygen levels at sub-micrometer spatial resolution, was based on fluorescence quenching of a ruthenium complex. The decrease in quenching was correlated to the oxygen concentration. A micrometer sized fiber optic glucose biosensor was developed by Rosenzweig and Kopelman, in which glucose oxidase and the ruthenium oxygen indicator were trapped within the gel on the fiber tip [6]. The sensor utilized a well-known detection scheme, in which glucose oxidase turned glucose into gluconic acid while consuming oxygen. The signal of the ruthenium complex would decrease as the oxygen was depleted from the surrounding solution. The sensor was 100 times smaller than current glucose sensors, and it had a response time of 2 seconds, which was comparable to existent needle-type amperometric sensors [7]. Moreover, the optical detection scheme has several advantages including the lack of an electrical current between sensor and sample.

The refinement of the fiber optic biosensor is partially due to improvements that have been made on the immobilization of the sensing components. Even though there are many different ways a variety of biomolecules (enzymes, antibody, antigen, proteins and DNA) [8,9-13] have been immobilized for sensor application, the majority of the solid supports cannot be used to study cellular or subcellular biological processes. One widely used method of immobilization of enzymes is the covalent binding to glass supports. This simple and optical straightforward method generally results in a high efficiency of binding and the maintenance of most activity. The most common covalent immobilization method used to adhere biomolecules to a sensor surface, be it capillary, microchip or fiber optic, is with the aid of membrane layers such as poly(acrylamide), phosphorylated polyvinylalcohol (PVA), lipid-protein matrix, protein films, polymer gels and zeolite modified surfaces [8,10]. These membranous layers create a type of cage trapping the working sensor biomolecule at the surface of the probe. A clear example of this technique was given above in Tan and Kopelman's work [5]. The surface of the fiber was photopolymerized, thereby trapping the biomolecule. However, covalent binding of biomolecules on an optical fiber surface is a difficult task. Most silica surfaces do not have suitable reactive groups. Such groups, may be introduced by chemical surface modification such as silanization.

Silanization techniques give the benefits of quick, reliable, and low-cost methods of immobilization of enzymes onto glass plates to catalyze large-scale chemical reactions [14]. This process is commonly performed by the deposition of a silane layer [15]. The surface amino groups introduced by silanization may be used for covalent binding of biomolecules directly or indirectly as an anchor for further surface conjugation.

1.2 Scope of Research

The work in this thesis focuses on the combination of fiber optic technology, surface modification and bimolecule immobilization for the fabrication and characterization of two specific fiber optic probe biosensors. We have taken the fairly new concept of fiber-optic biosensors, and combined it with several different approaches to resolve certain key issues. We have miniaturized the fiber optic probes by either pulling [1] or etching [16] to prepare sub-micrometer biochemical sensors for *in vivo* mapping of neurotransmitter release. A probe size in the sub-5 micrometer range should be sufficient for initial mapping experiments on the single cell level. Direct covalent immobilization of biomolecules to the optical fiber surface was accomplished through a new optical sensor fabrication technique using covalent binding mechanisms. None of the direct or indirect physical confinement methods, such as gel trapping or membrane immobilization, have been used for the sensor preparation. The optical fiber surface was initially activated by silanization. A functional cross-linker was used to conjugate the biomolecule to the surface of the fiber tip. The specific immobilization and reaction conditions of each sensor will be discussed. The detection limits of the miniaturized glutamate sensors have been tested in polycarbonate membrane wells. These sensors can be applied to the study of subcellular level neurophysiological responses.

CHAPTER 2
GLUTAMATE AND GABA

2.1 Role As Neurotransmitters

The basic unit of communication in all nervous systems is the neuron. The neuron is typically long and slender with two types of processes extending from either end. The *dendrites* are viewed as the input zones where the neuron receives and integrates information. The *axons* receive this information via an electrical signal through the neuron, resulting in signaling molecules being sent from the output zones, through the synaptic cleft, to another cell. The signaling molecules or ions are known as neurotransmitters. A number of substances have been thought to act as transmitters in the nervous system. Of particular interest are the amino acids glutamic acid (Glu) and γ-aminobutyric acid (GABA). In minute concentrations, they have been found to exert an excitatory and inhibitory effect, respectively, on neurons. Defects in the signaling process of these transmitters, whether it is release from axons or uptake from the dendrites of the neurons, are believed to lead to numerous diseases such as ischemic stroke, epilepsy, or Huntington's Chorea [17]. This picture of neuronal function is a simple explanation of an integrated and complex system. It is therefore necessary to understand, at greater detail, the roles that each neurotransmitter plays.

The main focus of this research is the fabrication of sensors that may detect glutamate and GABA in the signaling process of neurons. Glutamate plays a dominant role as a fast excitatory transmitter in the central nervous system. Beyond its primary function in excitatory synaptic transmission, glutamate acting at the synaptic level is also linked to neuronal development and degeneration. Glutamate levels in the synapses have been implicated in the neuronal damage related to ischemic stroke. It interacts with receptors that can be divided into two broad classes: NMDA (N-methyl D-aspartate) receptors, which are typical fast-acting directly coupled receptors that are permeable to monovalent cations; and non-NMDA receptors, which are both ligand-activated and voltage dependent. Activated by glutamate, the NMDA channels open allowing calcium ion influx, which can trigger calcium dependent second messenger systems in the postsynaptic cell. Ischemic cell death is thought to occur when there is an abundance of this second messenger (i.e. glutamate) in the post synaptic cleft, causing a high calcium influx, the accumulation of which leads to cell swelling and necrotic death. Upon cell death, there is lysis of the cell and release of its contents, namely glutamate. This abundance of glutamate in the extracellular fluid causes a cascade effect from one neuron to the next, destroying consecutive neurons, programmed cell death, until stroke occurs. Understanding this process is key to clarifying the complicated nature of glutamate action during physiological and pathological states in the central nervous system.

The GABA neurotransmitter system is of particular interest because of its important role in maintaining neuronal inhibition. Universally, GABA is known to inhibit neuron firing, both presynaptically and postsynaptically thereby affecting the Ca^+ and K^+ conductance of the cells. A decrease of GABA, and hence a decrease of neuronal inhibition, in the central nervous system has been linked to epileptic attacks and Huntington's Chorea [16]. When there is decline of GABA inhibition, there is continued depolarization of the neurons. When the cell is depolarized to a sufficient degree and duration, the Mg^+ that normally blocks the NMDA channel is removed, allowing Ca^{2+} to flow through these channels. The end result of prolonged depolarization is cell death. Epilepsy causes injury because of this prolonged depolarization and the events it triggers. A fuller understanding of the effects GABA concentrations hold on neurotransmission will advance anti-epileptic drug development. In addition, Huntington's Chorea Disease, a recently diagnosed neurological disease, like others, will benefit greatly from this technology.

2.2 Current Methods of Detection

The sensitive detection of neurotransmitters is of great interest in a variety of areas of biomedical research and biotechnology. There have been many research activities in the development of advanced bioanalytical techniques for the monitoring of a variety of biomolecules [7-9, 18-28], including glutamate and GABA, two substantially important neurotransmitters. The major techniques for sensitive glutamate detection are microelectrodes [7, 18, 28], fiber optic sensors [21, 22] and separation techniques coupled with optical or electrochemical detection [23-25]. These techniques have been useful for a variety of applications in glutamate monitoring. Using CE with laser-induced fluorescence detection, glutamate can be monitored at the 10^{-8} to 10^{-9} M levels [24, 25]. Smaller enzyme electrodes have been developed with high sensitivity, fast response time and excellent specificity for glutamate and lactate detection [7]. Direct measurement of glutamate release in the brain using a dual enzyme-based electrochemical sensor was developed. The enzyme-based electrode had a response time of about 1 s and a sensitivity of less than 2 μM. The microelectrodes had a size of a few micrometers. They were used for in-vivo monitoring of glutamate release from neurons induced by drug stimulation [1].

The major technique for GABA detection and quantification includes pre-/post column derivitization with capillary liquid chromatography and electrochemical detection [29, 31]. Conventionally, GABA has been determined by UV spectrophotometry, which is based on the change in absorption of compounds formed during incubation of the reaction mixture by the action of the enzyme system GABAse on GABA [30]. This process involved drawing samples from the extracellular fluid (ECF) of brain slices. Another technique used, which required drawing solution from ECF, was the bioluminescent assay [32]. These above techniques were useful for off-line monitoring of GABA but currently there is a need for analytical biosensors to be on-line for the continuous monitoring of concentration changes directly at the site of neurotransmission in real-time. Recently, an enzyme-based small-volume on-line electrochemical sensor was developed for the continuous measurement of GABA [28]. The sensor exhibited a sensitivity of 1.56 nA/μM for GABA, a detection limit of 0.1 μM within a linear range of 0.1 – 10 μM, and good selectivity for GABA when other biomolecules were present. The authors have not yet applied the system to a biological sample, but the results suggested that the sensor was capable of this function.

2.3 Enzyme-based Fluorescent Optical Fiber Probe

A biosensor comprises two principal components: a biological system which recognizes the analyte and responds to analyte concentration with an overall physiochemical change, and the transducer element which converts this change into an amplifiable and processible signal. The biological system that is the responsive component is normally an enzyme, or other biomolecule, that has a unique affinity and response based on the presence of a single analyte. There are specific enzymes that react to the presence of glutamte and GABA by the fluorescent end-product of their reaction, (NADH or NADPH). By using laser-induced fluorescence, we were able to detect NADH and NADPH at low concentrations (down to 10^{-8} to 10^{-9} M).

The enzyme glutamate dehydrogenase (GDH) can be used as a biosensor to carry out glutamate analysis in which the fluorescent NADH produced from the following reaction is detected:

$$\text{glutamate} + NAD^+ + H_20 \rightarrow \alpha\text{-ketoglutarate} + NH_4^+ + H^+ + NADH \qquad (2.1)$$

There has been some concern raised over the issue of the detection power of the sensor when only GDH is used as the detection enzyme in a sensor for glutamate detection [21]. Arnold and coworkers used two enzymes, GDH and glutamate-pyruvate transaminase, to prepare their 6 mm size optical fiber glutamate sensor [21]. The equilibrium constant for the GDH catalyzed reaction with NADH as the product is about 10^{-14} M^2 [33], which constitutes a thermodynamic barrier to the production of NADH. Therefore, the detection of glutamate at very low concentrations may be difficult. However, this should not become a major problem when the glutamate concentration is in the micromolar to submicromolar range. Our calculations have shown that the thermodynamic equilibrium is still favorable for the production of NADH when the reaction proceeds under the following conditions: [glutamate] = 0.1 μM, [NADH] = 0.1 μM, [NAD^+] = 1 mM and pH=7.4. The reaction quotient, (K_{eq}), at these concentrations is about 10^{-19} M^2, supporting the suitability of these conditions for glutamate detection at the submicromolar range. Therefore, the reaction proceeds to the production of NADH even when the glutamate concentration is as low as 5×10^{-8} M. It is known that static extracellular glutamate is in the micromolar concentration range and the released glutamate from a cell is in the millimolar range prior to diffusion from the cell [17, 34].

The enzyme system, GABAse is more complex then GDH because it is an enzyme *system* composed of two enzymes, γ-aminobutylate ketoglutarate aminotransferase (GABA-T) and succinic semialdehyde (SSDH) [35]. Together they catalyze the following reactions:

$$\text{GABA} + \alpha\text{-ketoglutarate} \xrightarrow{\text{GABA-T}} \text{succinic semialdehyde (SSA)} + \text{glutamic acid} \quad (2.2)$$

$$\text{SSA} + \text{NADP}^+ + H_2O \xrightarrow{\text{SSDH}} \text{succinate} + \text{NADPH} \quad (2.3)$$

This system in the presence of GABA and α-ketoglutarate will result in a detectable signal from NADPH.

Enzymes are extremely effective catalysts. They exhibit a very high substrate- and stereospecificity. These properties make enzymes extremely attractive tools for use as biosensors.

2.4 *In-vivo* Issues of Glutamate and GABA Detection

The first goal of this research was the development of a glutamate biosensor suitable for continuous monitoring of glutamate release from individual cells or subcellular structures, thus resulting in an effective detection technique for *in-vivo* mapping of extracellular glutamate concentration. Subsequently, the idea for a comparable GABA biosensor soon followed due to a similar need for an effective detection technique for the *in-vivo* mapping of extracellular GABA concentration. *In vivo* mapping of the rapid changes in extracellular glutamate and GABA concentrations in a cell culture during insult has not been possible due to the limitations of available analytical techniques. Current techniques for the measurement of the release of endogenous glutamate and GABA into the extracellular space of the central nervous system are relatively slow and have inadequate spatial resolution. Continuous monitoring of the extracellular glutamate and GABA release will permit the resolution of the kinetics of neurotransmitter release. However, this can be realized only if the analytical probe in the extracellular space is sufficiently small, very specific, highly sensitive and fast. In order to map extracellular glutamate and GABA concentration changes during ischemia or epilepsy, the detection technique must have high sensitivity (down to micromolar concentration), fast response time (shorter than 1 s) and excellent spatial resolution (submicrometer to about 5 μm).

2.5 Summary: Why use Micrometer Fiber Probes?

Near-field optics (NFO) employing optical fiber probe sensors should be best suited for the mapping of extracellular glutamate and GABA concentrations. Previous optical fiber glutamate sensors have been successful for glutamate detection at submicromolar levels [21, 22]. Glutamate sensors were prepared by using either a membrane or acrylamide gel to trap glutamate dehydrogenase (GDH) and other enzyme molecules [27]. The glutamate sensors were stable, reproducible and selective. However, they cannot be used for *in-vivo* monitoring due to their large size (a few millimeters to a few hundreds of micrometers) and long response times (4 to 8 minutes [21]). Recent developments in submicrometer optical fiber sensors [5, 36-38] should easily allow for preparation techniques of sensor probes that are sufficiently small for studies in microscopic regions. Photo-nanofabrication and chemical etching are preparation techniques for ultra-small and ultra-fast biochemical sensors [5, 16]. However, in order to have biomolecules, such as GDH or GABAse, covalently bound directly to an optical fiber probe, special functional groups are required. New techniques must be developed for biomolecule immobilization that will aide in creating biosensors with excellent sensitivity and fast response times.

CHAPTER 3
EXPERIMENTAL CONSIDERATIONS

3.1 Instrumentation

3.1.1 Experimental Set-Up

The experimental set-up for the GDH enzyme probe and GABAse probe characterization was based on an inverted Olympus fluorescence microscope (model IX708F). In this apparatus, shown in Figure 3.1, the fluorescence microscope was connected to an avalanche photon diode (APD) (SPCM-200 CD 2027, EG&G, Quebec, Canada) through the side port of the fluorescence microscope to minimize stray light interference. The excitation source was a multi-line UV (MLUV) Innova 90 Ar^+ laser (Coherent Laser, Santa Clara, CA). A high precision single mode fiber coupler from Newport Corp. was used to direct the laser beam into an optical fiber splice (CamSplice, Siecor). The bare end of a GDH immobilized or GABAse immobilized optical fiber was coupled to the excitation source. The fluorescence was collected via a quartz microscope objective. The higher the numerical aperture of the objectives used for collection, the larger the signal collected. The objective lens transmits in the UV range of 300 to 400 nm, and has limited autofluorescence. The NADH and NADPH luminescence was transmitted by a dichoric mirror through a 420 nm long pass filter, a 465 nm interference filter (Oriel Corporation, Stratford, CT) and subsequently directed into the APD system. The signal was amplified by a DC-300 MHz amplifier model SR445 (Stanford Research Systems, Sunnyvale, CA). An EG&G ORTEC MCS-Emulator was used to process the fluorescence intensity data as a function of time. For well-controlled vibration isolation, the entire microscope based set-up was on a laser table. Each new fiber was fastened to the stage of the microscope and viewed before data collection.

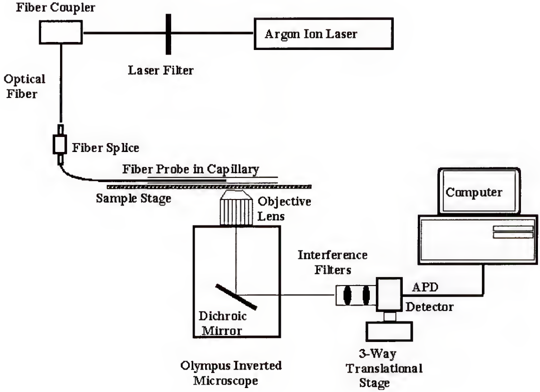

Figure 3.1 Schematic diagram of the optical set-up for enzyme probe measurements.

3.1.2 Microscopic Probe Imaging.

We have also designed and constructed an experimental set-up for collecting images of NFO probes, measuring the light throughout of our tips, and viewing of the fluorescence produced by NADH under laser excitation. It is similar to the set-up for the fluorescence measurements described above; however, in this apparatus, the inverted frame fluorescence microscope (IX708F, Olympus) was connected with a frame transfer CCD camera (RTE/CCD-512EFT, Princeton Instrument, Inc., Trenton, NJ). The CCD camera was mounted on the top entry port of the microscope, facing downward. A 488-nm laser beam from an Ar^+ laser (Model 532-100A, Omnichrome, Chino, CA) was used for excitation of the NADH and NADPH measurements. The fluorescence was collected via quartz microscope objectives with a 40X magnification. The objective transmited in the UV range of 300 to 400 nm, and had a negligible autofluorescsence. The fluorescence was transmitted by a dichroic mirror and subsequently directed into the CCD camera. In front of the CCD camera, longpass and interference filters were used to collect selectively the desired fluorescence. The entire microscope based set-up was on a laser table for well controlled vibration isolation.

The submicron fiber sensors were also positioned using an Eppendorf Micromanipulator 5171, Madison WI, into microwells for detection limit measurements. The 5 µm wells in polycarbonate membranes, "Nucleopore", used to hold the substrate solution, were mounted on a microscope cover-slip. Some of the submicron fibers were pulled to nanometer diameters with a P-2000 puller from Sutter Instrument Co., Novato, CA.

3.2 Reagents and Materials

L-glutamic dehydrogenase (E.C.1.4.1.3, 43 units mg^{-1} protein from bovine liver) and N-methyl-D-aspartic acid (NMDA) were purchased from Sigma Chemical Co.. GABAse was purchased from Boehringer Mannheim, Germany. L-glutamic acid (monosodium salt monohydrate)(glutamate), γ-aminobutyric acid (GABA), α-ketoglutarate (α-KG), NAD$^+$, NADH, NADP$^+$, succunic semialdehyde (SSA), glutaric dialdehyde (25 wt % solution), 3-aminopropyl triethoxysilane, fluoreascamine, and all amino acids used in the physiological interference study were purchased from Acros Organics, Fairlawn, NJ. Trimethoacysilylpropyldiethylenetriamine (DETA) was purchased from United Chemical Technologies, Bristol, PA. Optical fiber with core diameters of 105 or 50 μm was obtained from General Fiber Optics, Inc. (Fairfield, NJ), and single mode optical fiber with core diameter of 3.5 μm was from Newport Corp.. Submicrometer to micrometer optical fiber probes were prepared by hydrofluoric acid etching[39].

3.3 Procedures

3.3.1 Pulling and Etching Optical Fiber Tips

The Sutter P-2000 Micropipette Puller containing a CO_2 infrared laser was used to produce optical fibers that tapered to form tips ranging from 0.1 to 1 μm in diameter [5, 6]. Tips were also made by chemical etching in 40-50% hydrofluoric acid solution. Our chemical etching technique involved the use of an organic or oil layer on the surface of the hydrofluoric solution as the protective layer. Denuded optical fiber ends were immersed in the HF solution containing a protective organic solvent. The protective layer formed a meniscus at the liquid-liquid interface when the fiber was immersed into the solution. As etching progressed, the meniscus decreased with time as the diameter of the fiber end decreases. This produced the taper which eventually formed the tip.

3.3.2 Optical Fiber Probe Surface Modification

Batches of 6 to 10 optical fiber probes, were used in a single immobilization cycle. The fiber tips were first cleaned by immersion in 1:1 concentrated HCl:MeOH for 30 minutes. They were then rinsed in deionized water and submerged in concentrated H_2SO_4 for 30 minutes. Further rinsing and then boiling in deionized water for 8-10 minutes followed. Silanization of the fibers was performed by immersion in freshly prepared 1% (v/v) solution of distilled DETA in 1 mM acetic acid for 20 minutes at room temperature (23^o C). The DETA-modified fiber tips were thoroughly rinsed with deionized water to remove excess DETA. The silanized fiber probes were dried under N_2 and fixed with heat in a 120^o C oven for 5 minutes.

Conjugation of the tips was carried out using the bifunctional crosslinker, glutaraldehyde. A condensation reaction of glutaraldehyde carboxyl groups to the amino groups on the fiber's surface formed carboamides. The silanized tips were kept in a 12.5% (v/v) glutaraldehyde solution with 0.1 M potassium phosphate buffer solution (PBS) at pH 6.8 for 14 hours at room temperature.

Fluoresceinamine is intrinsically a nonfluorescent compound, but reacts in milliseconds with primary aliphatic amines to yield a fluorescent complex as shown in Figure 3.2. It was employed to detect the amino groups on the tip surface. The silanized tip was immersed in 1mM fluoresceinamine-DMF solution for 4 to 60 minutes. Fluorescamine was subsequently used to confirm the binding of the glutaraldehyde to the aminosilane layer. A lack of fluorescence was a positive response.

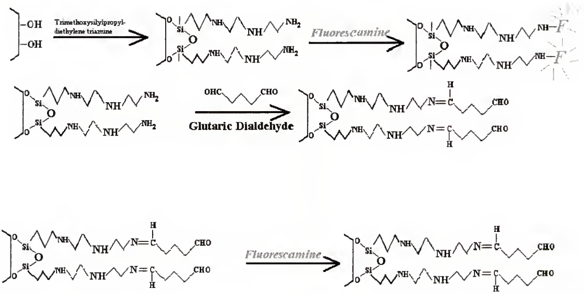

Figure 3.2 Detection of primary amines on the fiber surface before conjugation.

In the next step, it was particularly critical to remove all excess glutaraldehyde before placing the tips into the enzyme solution for immobilization [9]. Therefore, meticulous rinsing with deionized water and complete drying under N_2 was performed after conjugation. The unreacted carboxyl termini of the bifunctional crosslinker were left for the linking to the primary amines on the target enzyme, as illustrated in Figure 3.3.

3.3.3 Enzyme Immobilization - GDH.

The GDH enzyme solution concentration of 1 x 10^{-5} M was prepared in 0.1 M PBS at pH 6.8. The fiber tips were immersed in GDH solution for 5 to 29 hours at room temperature to allow the enzymes to be immobilized on the surface. The tips were subsequently washed with buffer, and either used immediately or stored in PBS at 4° C when not in use. For miniaturized optical fiber probes, special care was taken to only allow the surface of the probe touch the enzyme solution. GDH was mainly immobilized at the end surface of the miniaturized fiber tip surfaces.

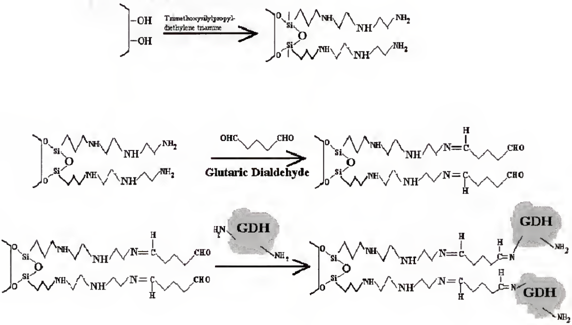

Figure 3.3 Immobilization of glutamate dehydrogenase on a fiber optic surface.

3.3.4 Enzyme Immobilization - GABAse.

The GABA biosensors were prepared by immersing conjugated tips into a solution of approximately 1.0 mg/ml of soluble GABAse in PBS buffer at pH 6.8. The fibers where immersed in GABAse solution for 5-29 hours at room temperature to allow the enzymes to be immobilized on the surface. The tips were subsequently washed with buffer, and either used immediately or stored in substrate solution in the freezer when not in use.

3.4 Sensor Response Analysis

Measurement of the immobilized enzyme activity was carried out within the 300 μm inner diameter capillary tubes called nanoscopic enzymatic reactors. The enzyme probe was inserted into a clean capillary and stabilized to the microscope stage so that the very tip of the GDH immobilized optical fiber was in focus at the objective lens (Figure 3.4). The fixed probe was rinsed by injection of PBS buffer solution through the opposite hole of the tube. A substrate solution in PBS (pH 8.0) of a known amount of either: glutamate and NAD^+ or GABA, α-KG, and $NADP^+$, was injected into the capillary. The production of NADH or NADPH and subsequent fluorescence was recorded by the APD based detection system. NADH and NADPH fluorescence was measured as a function of time. The dwell time on the APD could be as short as 1 μs for each measurement. Following each substrate injection, the capillary and the enzyme probe were rinsed with fresh aliquots of PBS to restore a baseline signal. All experiments were carried out at room temperature (23° C). The reaction rates were calculated based on the raw data of the NADH or NADPH fluorescence intensity vs. time. Both initial reaction rates and steady-state reaction rates were used for sensor characterization.

3.4.1 Measurements in Pre-formed Membrane Wells

To isolate micro-scaled volume of substrate in the attoliter range, 5 μm diameter microwell polycarbonate membranes fixed on a coverslip were used to measure the submicron pulled or etched enzyme-immobilized fibers. These wells simulated measurements that would be taken at the level of a biological cell. Before testing, the membranes were placed in substrate solutions, and vacuum was applied to pull the solution into the wells. Once a membrane was placed on the coverslip and on the microscope stage, the fiber was driven by the micromanipulator into one of the holes and the reaction fluorescence was collected. The detection limits of the biosensors were measured in the wells.

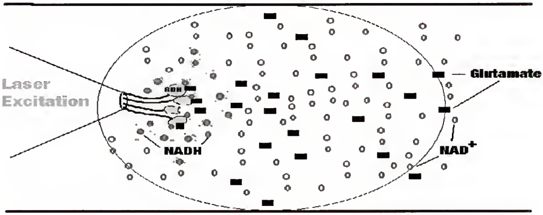

Figure 3.4 View through the objective lens after injection of the capillary with substrate.

CHAPTER 4
FABRICATION AND CHARACTERIZATION OF THE GLUTAMATE SENSOR

4.1 Results and Discussion

4.1.1 Direct Covalent Immobilization of GDH on Optical Fiber Surface.

GDH enzyme molecules can be directly immobilized onto an optical fiber surface by covalent binding. The immobilized GDH molecules have excellent enzymatic activities. The detailed molecular immobilization mechanism is shown in Figure 3.3. This mechanism is a novel combination of several surface modification techniques [9-12] specifically designed for our sensor preparation. Proper surface preparation is essential for optimal GDH immobilization. The surface must be cleaned of any interference to assure maximal exposure of hydroxyl groups on the silica fiber. The aminosilanes on the fiber surface can support crosslinker modification and subsequent biomolecule attachment. DETA was found to be more reliable among the silinazation agents tested. Silanization of the fiber's surface by DETA was confirmed by reacting the silanized fiber tip with fluorescamine [40]. Fluorescamine is intrinsically a nonfluorescent compound, but reacts in milliseconds with primary aliphatic amines to yield a fluorescent complex. Thus, it can be employed to detect the amino groups on the tip surface. Conjugation of GDH is carried put by the use of glutaraldehyde, where one carboxyl group reacts with an amine from the aminosilane layer on the fiber and the other carboxyl group reacts with the amine-containing biomolecules. Glutaraldehyde was used as the line of attachment from the tip to the biomolecule. The linker serves two important functions to our sensor, namely to covalently bind two distinct chemical entities which otherwise would not react with one another and to act as a spacer arm allowing for greater accessibility and/or freedom to the attached biomolecule. This freedom, allowed through cross-linking, is essential to the activity of the enzyme molecules reacting with its substrate. Cross-linking differs from the membranous layer and film techniques in that the enzyme molecule is out in the solution versus in a matrix of a membrane. Once the probes were properly treated with silanization and cross-linking, they were inserted into a GDH buffer solution for GDH immobilization. GDH concentrations were maintained in the range of 10^{-5} to 10^{-7} M for all fibers. All immobilization experiments of the GDH enzyme took place at the optimal pH 6.8, PBS. Increased enzymatic activity of the probes incubated in GDH at 25° C versus 4° C was found. The length of time a 1×10^{-5} M GDH solution was incubated with the fibers was varied from 90 minutes to 35 hours. The GDH probe thus prepared have shown enzymatic activities when tested with glutamate and NAD^+.

4.1.2 Effect of Immobilization Time on GDH Probe's Activity.

The duration of the GDH molecules' immobilization onto the treated optical fiber probes was studied. To achieve high activity of the GDH probe for the catalytic reaction between glutamate and NAD^+, an effective form of GDH is required. In addition, adequate amounts of GDH have to be immobilized onto the limited fiber surface area. As shown in Figure 4.1, the maximum activity for the probe occurs between 20 and 25 hours of immobilization in GDH, although even after 2-hour immobilization in GDH solution, there is a measurable NADH production. Two different ways of characterizing enzymatic activity have confirmed this result. The first one involved the absolute increase in NADH signal produced in a given time, while the second made use of the enzymatic reaction rate. Both confirmed the trend shown in Figure 4.1. It is noteable that the 25-hour immobilization time is the time used for the GDH probe preparation; however, the time is varied depending on the specific experimental conditions. The reason for the decline in activity after 25 hours in GDH solution is not known. Possible reasons include double GDH layer formation and enzyme molecular conformational changes.

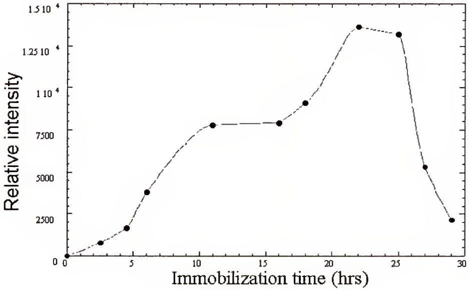

□

Figure 4.1 Effect of immobilization time on the sensor response. NAD^+ and glutamate concentrations were 1mM and 4mM, respectively.

4.1.3 NAD^+ and Glutamate Affect on GDH Immobilization.

There are reports on the effect of substrate co-immobilization on the enzyme molecule's activity [10, 27]. The co-immobilization of GDH with either glutamate or NAD^+ was measured. Both NAD^+ and glutamate have free amine groups. Three sets of experiments were carried out to study the immobilization of GDH molecules. In the first experiment, the surface treated fiber probe was inserted into a 4 mM NAD^+ solution for 20 hrs and then was put in a GDH solution for further GDH immobilization. In the second experiment, NAD^+ was replaced by glutamate, and all three compounds were in the same solution for co-immobilization in the third experiment. The activities of the enzyme probes prepared in these three experiments were about the same as that obtained from a probe prepared by GDH immobilization alone.

4.1.4 NAD^+ Affect on Glutamate Sensor Performance.

The GDH sensor activity is shown in Figure 4.2 as a function of NAD^+ concentration (0 to 5 mM). When the concentration of NAD^+ was increased, the sensor responded in an asymptotic approach to maximum enzyme activity. The GDH activity on the probe is nearly independent of the co-substrate when the concentration of NAD^+ is above 1 mM. The concentration of NAD^+ used in all subsequent experiments was 1 mM.

4.1.5 GDH Probe for Sensitive Glutamate Detection.

The GDH optical fiber probe is an effective sensor for glutamate detection down to the sub-μM range. The glutamate response curve obtained under optimal conditions is shown in Figure 4.3. Reaction rates were used to characterize the sensor's sensitivity in monitoring glutamate concentration changes. Initial reaction rates were calculated using the first 200 data points (25 ms dwell time at each point) in continuous monitoring of the production of NADH at different glutamate concentrations. The reaction rates of GDH versus glutamate concentration (0 to 18µM) are shown in Figure 4.3. The detection limit of our glutamate sensor is 0.2 µM, which is adequate for measurements taken at the physiological level of subcellular release (typically in the mM range). A reaction rate to characterize the detection limit of the glutamate sensor is more appropriate than measurements of steady-state NADH fluorescence intensity. Usually a few minutes were required to reach a steady-state depending on the concentrations of glutamate [21]. The reaction rate is an instantaneous measurement which is solely dependent on glutamate concentration under optimal conditions.

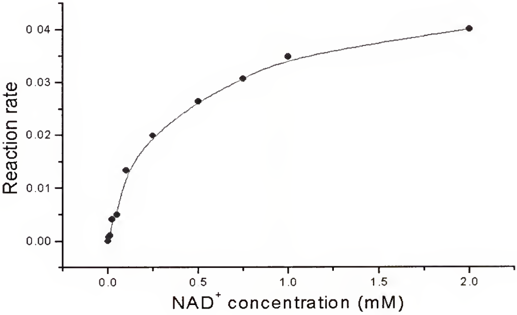

Figure 4.2 Effect of NAD$^+$ concentration on the glutamate sensor activity.

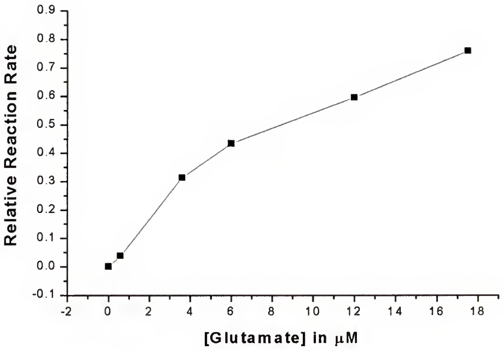

Figure 4.3 Glutamate calibration plot using a GDH probe with NAD^+ concentration at 1mM.

Compared with previous reported state-of-the-art optical GDH enzyme probe [21] and other surface immobilized optical sensors, the GDH probe prepared in this work is much smaller in sensor diameter and thus in sensing area. In addition, only one enzyme is used for the preparation of this glutamate sensor. However, the sensitivity of the GDH probe is comparable with what has been reported for a glutamate optical sensor with a few millimeters in size. There are two possible reasons, which contribute to the high sensitivity of the present glutamate sensor. First, the present sensor involves is the direct immobilization of GDH molecules on the fiber surface without membrane, gel or any other carriers. The analyte has direct access to the GDH molecules. Moreover, the present design leaves a large free space between the fiber surface and the GDH molecules through long chains. Thus, the GDH molecules are effective in their activity, catalyzing the reaction between glutamate and NAD^+. Second, the present sensor has a high efficiency of detection.

4.1.6 Glutamate Sensor Stability and Selectivity.

The stability of immobilized GDH was tested for its ability to withstand multiple use over time (see Figure 4.4). Measurements were taken every 2 hours over an eight-hour period to simulate one typical working day. The sensors were then stored at 4^o C overnight and evaluated each day for 3 days. The sensor retained approximately 85% of its original activity after 3 days. Due to the fragility of a single optical fiber sensor, it was relatively difficult to collect data after three days of usage and storage. Optimal storage conditions were found to be at 4^o C. Although some data showed excellent enzymatic activity after storage at 25^o C in dry air, we believe that 4^o C in a buffer solution are the best conditions for maintaining the GDH's enzymatic activities.

GDH is highly selective in the deamination reaction for glutamate compared with other substrates. The selectivity of the GDH sensor probe for its substrate was demonstrated by attempting to report any response to compounds common to neurochemical or physiological media (see Figure 4.5). The measure of the response was compared to that obtained using 17.5 μM glutamate. As shown in Table 1, high millimolar concentrations of potential interferences had little or no effect upon the activity of the GDH sensor. Ascorbate and cysteine initiated a small response. Potential interference from NMDA was also evaluated. NMDA is often used as a drug to stimulate cellular release of glutamate from a neuron [34]. NMDA is structurally similar to glutamate, and could very possibly lead to a false response when applying the GDH sensor to cellular studies. Under our experimental conditions, there was no detectable sensor response when exposed to NMDA.

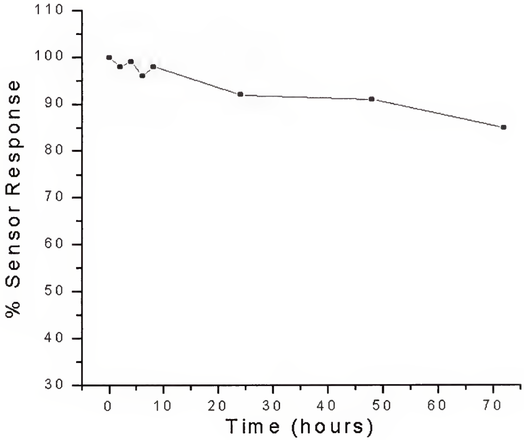

Figure 4.4 Response to 1mM glutamate and 4mM NAD^+ as a function of sensor age.

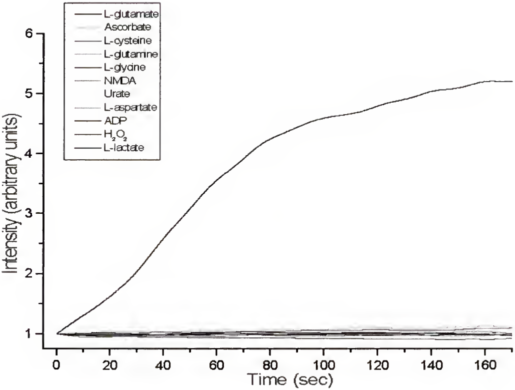

Figure 4.5 Selectivity of GDH probe for glutamate over physiological interferences.

Table 1: Relative Response From Potential Physiological Interferences

Compd	% response	compd	% response
L-glutamate	100	L-glycine	0
ADP	0	H_2O_2	0
L-ascorbate	2.0	L-lactate	0
L-aspartate[3]	0	NMDA[1]	0
L-cysteine	1.6	urate[2]	0
L-glutamine	0		

4.1.7 Glutamate Sensor Response Time.

The response times of two separate GDH fiber sensors are shown in Figure 4.6. To ensure of maximum sensor response, NAD^+ and glutamate concentrations were 1 mM and 1 mM, respectively. Our probes have response times less than 50 ms. The response time for the glutamate sensors in this paper is defined as the time required for the GDH probes to generate sufficient NADH for detection. The shortest response time of the sensor corresponds to the minimally required optical signal generated by NADH. The standard deviation of the background is used to estimate the response time of the sensor (3σ, σ = standard deviation). This definition of response time for enzyme based sensors is well suited for the intended application of the sensors. When a biological cell releases glutamate, the speed at which the sensor can detect the released glutamate is an important characteristic property of the sensor. Response time determines the suitability of the sensor's application to a specific problem of study. A great benefit to our GDH biosensors is the minimal recovery time needed. Usually, there is a period of time required for other sensors to reach baseline conditions. The GDH biosensors prepared in this work were ready for experimental measurements directly after rinsing with PBS buffer.

4.1.8 Submicrometer Glutamate Sensors.

The direct immobilization method used in the sensor preparation enabled miniaturization of the glutamate sensor to the submicrometer scale required for subcellular monitoring. The submicrometer sensor can easily detect a glutamate concentration of 3.6 μM in our capillary based enzyme reactor, as shown in Figure 4.7.

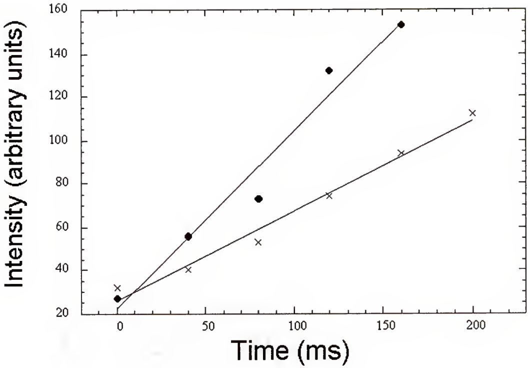

Figure 4.6 Response of two GDH probes are shorter than 50 ms. NAD$^+$ and glutamate concentrations were 1mM and 1mM, respectively.

To determine the absolute mass detection limit of the submicrometer glutamate sensor, a 5 μm diameter polycarbonate membrane holes with a depth of about 10 μm [41] was used for ultrasensitive glutamate detection. These membrane holes were similar to single biological cells in size, shape and dispersion on the surface. The glutamate sensor was inserted into one specific hole which was filled with the substrate solution, as shown in Figure 4.8. The fluorescence intensity from this hole was monitored as the probe was inserted. Glutamate concentrations down to 15 μM were detected, giving our sensor an absolute mass detection limit of about 3 attomoles of glutamate. The concentration of glutamate in the volume of one microwell was used to calculate the limit of detection. This experiment imitated in-vivo cellular monitoring, in which a glutamate sensor is positioned over cell membrane. We have also confirmed that the sensor is useful in preliminary single cell monitoring of glutamate release.

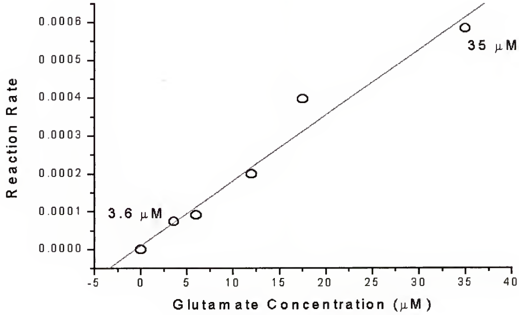

Figure 4.7 Glutamate calibration plot using a 5μm etched GDH probe. NAD$^+$ was 1mM.

4.2 Conclusions

Ultrasensitive glutamate optical sensors, with micrometer to submicrometer sizes, have been developed by directly immobilizing glutamate dehydrogenase molecules onto optical fiber probe surfaces through newly developed covalent binding mechanisms. New immobilization procedures, including tip silanization, conjugation and chemical binding of glutamate dehydrogenase have been created to coordinate the enzyme molecules to the optical fiber tip. Optimal immobilization of GDH occurred between 20 and 25 hours in the enzyme solution. The glutamate sensor (105 μm to submicrometer in diameter) is small, uses only one type of enzyme molecule, is simple in its preparation, is easy to use and is fast. The glutamate dehydrogenase molecules on the optical fiber surface have high enzymatic activity. The sensor's detection concentration limit is 0.2 μM glutamate. The absolute mass detection limit is 3 attomoles for a submicrometer glutamate optical sensor. The detection system can monitor NADH generated by the sensor within 50 ms. The glutamate sensor is stable and extremely selective. The nano-scaled probes will be useful to study subcellular level neurophysiological response in glutamate release monitoring experiments.

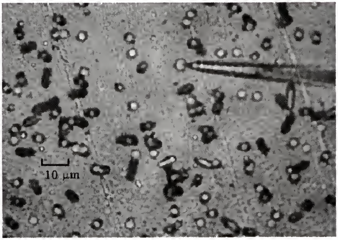

Figure 4.8 Glutamate monitoring in a 5 μm polycarbonate membrane hole by a submicrometer GDH probe.

CHAPTER 5
FABRICATION AND CHARACTERIZATION OF THE GABA SENSOR

5.1 Results and Discussion

5.1.1 Fluorescent Response of GABA

The GABAse enzyme probe proceeds on the fundamentals of an NADPH-based GABA biosensor [35]. Once the two enzymes are immobilized onto the surface of the fiber tip and the probe is fixed in the capillary enzymatic reactor, injection with GABA, α-ketoglutarate and $NADP^+$ results in diffusion to the enzyme layer on the tip's surface. At the tip surface, which is in the focal plane of the objective lens, GABAse catalyzes the transition of $NADP^+$ to NADPH through the oxidation of SSA (equations 2.2 and 2.3). The enzyme reaction increases the amount of NADPH at the surface of the sensor tip, while simultaneously increasing the signal of the sensor. A maximum NADPH signal is attained when the fluorescence radiation collected through the objective lens and detected by the APD, reaches a steady plateau over time. The initial rate of the NADPH fluorescence increase is related to the concentration of GABA injected into the capillary as long as the rate of NADPH production is in the pseudo-first order range with respect to the GABA concentration.

We are in the early stages of developing different methodologies for biomolecule immobilization on an optical fiber surface. The experimental variables for the immobilization process and optimized reaction conditions have been investigated. These variables of fiber surface preparation include cleaning methods, silanization time in DETA, conjugation time for the addition of the cross-linker glutaraldehyde and immobilization time of the two enzyme system onto the fiber surface. Other variables evaluated were possible enzyme activity enhancement with optimal pH conditions, concentration of $NADP^+$ and α-ketoglutarate, selectivity for $NADP^+$ over the more commonly used NAD^+, and GABA sensitivity.

Proper surface preparation is essential for optimal enzyme immobilization. The surface must be cleaned of any interference that could block space on the surface of the fiber and to assure maximal exposure of hydroxyl groups on the SiO_2. Since surface area of the tip is minimal, it is critical to have the maximum area for GABAse immobilization. The reaction of the enzyme occurs at the tip; therefore the excitation wavelength at the tip should be maximal for excitation of NADPH.

Cleaning and silanization procedures outlined in Chapter 3 were followed. Conjugation of biomolecules is very commonly accomplished through the use of glutaraldehyde, where one carboxyl group reacts with an amine from the aminosilane layer on the fiber and the other carboxyl group with the amine-containing biomolecules. Glutaraldehyde, a commonly used homobifunctional cross-linker, was chosen as the attachment mechanism between the tip to the biomolecule. The linker serves two important functions in the present sensor: first to covalently bind two distinct chemical entities which otherwise would never react with one another and second as a spacer arm allowing greater accessibility and/or freedom to the attached biomolecules (Figure 5.1). This freedom allowed through cross-linking is essential to the activity of the enzyme reacting with its substrate; this approach differs from the membranous layers and films techniques in that the enzyme is in the solution rather than in a matrix of a membrane. The reaction rate is not dependent on the diffusion time of the substrate through the film on the surface.

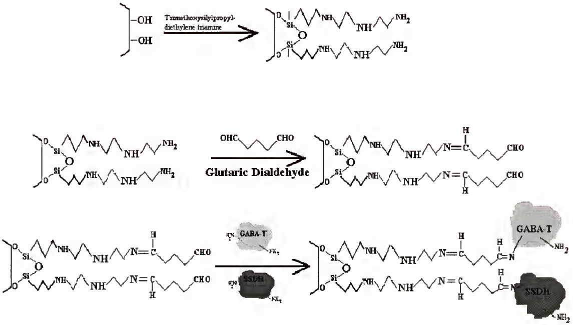

Figure 5.1 Immobilization of the two enzymes of GABAse on a fiber optic surface.

The conjugation of the homobifunctional cross-linker, glutaraldehyde, on the fiber surface was then verified by measuring the fluorescence after incubation of the fiber with fluoresceinamine. Since the entire aminosilane layer was bound to the glutaraldehyde, there was no place for attachment of fluoresceinamine. The lack of fluorescence was a good measure of conjugation.

The enzyme-modified fiber was compared to a bare fiber by measuring the response of immobilized GABAse to free GABAse in solution. In Figure 5.2a it can be seen that the present optical set-up detects responses with a bare fiber surface and GABAse in solution (1) in PBS containing GABA, α-ketoglutarate and NADP$^+$ in solution and (2) in PBS containing only α-ketoglutarate and NADP$^+$. In Figure 5.2b, a GABAse immobilized fiber surface responds to PBS solution (1) containing GABA, α-ketoglutarate and NADP$^+$ and in PBS solution (2) containing α-ketoglutarate and NADP$^+$. An increase in fluorescence intensity in th presence of GABA due to the production of NADPH, (refer to equations 2.2 and 2.3) is shown in both Figure 5.2a and b. There was no detectable increase in fluorescence in the absence of GABA indicating that there was no enzymatic reaction occurring. This clearly shows that there is an increase in fluorescence due to the activity of GABAse with GABA in solution or on the surface of the fiber. The fluorescence of NADPH collected at the surface of the fiber confirms the immobilization of the two-enzyme system on the fibers.

The response of the immobilized enzyme is shown in Figure 5.2a. It is evident that there is a very strong signal in the presence of the enzyme, although the reaction time of the immobilized enzyme is longer than the free enzyme. This could possibly result from the conformational changes of the enzymes occurring upon immobilization. Another possibility could be due to the reaction kinetics of the individual enzymes, GABA-T and SSDH, and the availability of the reactants as compared to the products. The initial production of glutamic acid could be large, which would reduce the rate of the first enzyme reaction due to end product inhibition. If the reaction rate is reduced, the SSDH may not have enough SSA to react with NADP$^+$, thereby retarding a detectable signal. The dramatic increase could occur at the point of saturation of the first reaction, at which time the second would take over.

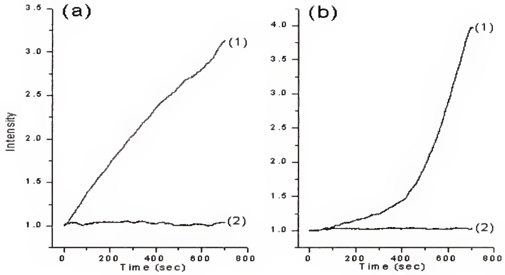

Figure 5.2 (a) 1. - Free GABAse in solution in the presence of 1mM GABA, α-KG and NADP$^+$. 2. - Free GABAse in the same solution as 1, but without GABA. (b) 1. - Immobilized GABAse in the presence of 1mM GABA, α-KG and NADP$^+$. 2. - Immobilized GABAse in the same solution as 1, but without GABA.

When optimizing the immobilization conditions of the GABAse enzymes, 105 μm core optical fibers silanized in DETA and conjugated with glutaraldehyde (pH 6.8) were used. Limiting GABAse amount on a small surface may have adverse affects to sensitivity and to the detection limit of the sensor. Therefore, we maintained GABAse concentrations in the range of 1 mg/ml for all fibers. All immobilization experiments of GABAse took place at optimal pH 6.8, phosphate buffer solution (PBS). Increased enzymatic activity of the probes occurred when incubated in GABAse at 25° C versus 4° C. The length of time a 1 mg/ml GABAse solution was incubated with the fibers was varied from 11 to 25 hours. The results shown in Figure 5.3 indicates the maximum activity for the probe occurs after 19 hours of immobilization in GABAse, although even after 11 hours in GABAse solution, there is a measurable fluorescence. The decline in activity after 22 hours in GABAse solution may be due to crystals formed on the surface of the fiber. These crystals were not seen through the microscope at or before 19 hours immobilization. There was a noticeable background increase in correlation with the formation of the crystals on the fiber. A possible reason for this increase may be the scattering of light due to the crystals.

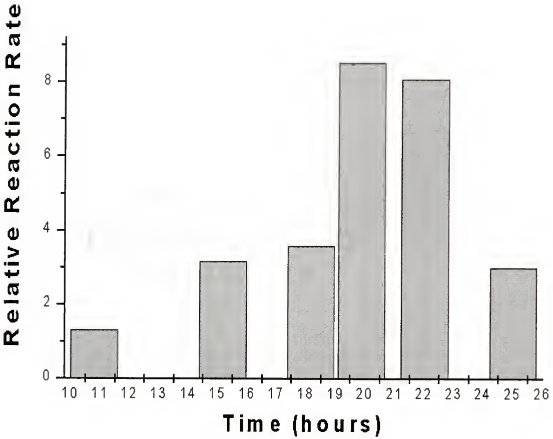

Figure 5.3 Effect of immobilization time on the sensor response. NADP$^+$, α-KG and GABA were 1 mM.

5.1.2 Influence of pH.

The influence of pH on enzymatic reactions has been studied extensively. It is known that the environment of a biosensor greatly effects its response. Figure 5.4 shows the relationship between the immobilized GABAse on the fiber and the pH of the reaction solution. The maximum activity occurred from pH 7.5 – 9.0. The reaction of SSA and $NADP^+$ catalyzed by SSDH releases H^+; therefore a high pH is advantageous to the forward reaction (equation 2.3). However, at high pH, there is a possibility of $NADP^+$ decomposition and enzyme instability. The optimum response of the GABA sensor was in accordance with the physiological range. This range is consistent with typical enzyme activity references.

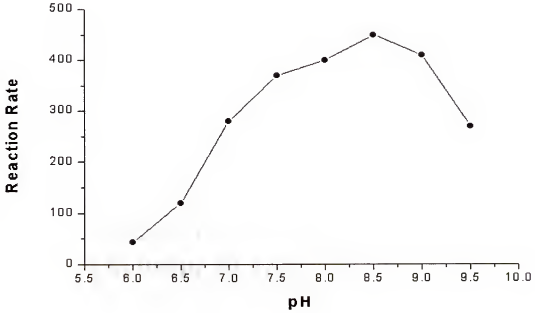

Figure 5.4 Influence of pH on the GABA fiber sensor. $NADP^+$ was 1 mM and α-KG and GABA were 100 μM.

A great benefit of the fiber optic GABA biosensor is the short recovery time needed. Usually, there is a prolonged period of time required for other sensors to reach baseline conditions. The present GABA biosensors were ready for experimental measurements immediately after rinsing with PBS, pH 8.5. The fluorescence intensity of NADPH rapidly decreased to baseline as the capillary reactor was injected with buffer. The return to baseline is shown in Figure 5.5. Subsequent signals can then be monitored after injection with fresh substrate solution.

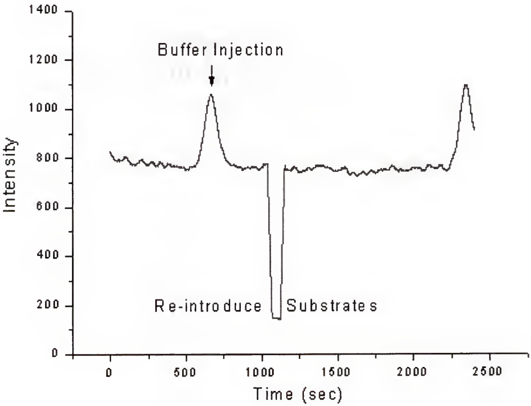

Figure 5.5 Minimum recovery time needed to eliminate fluorescence and begin new run. NADP$^+$, α-KG and GABA were 400 μM.

5.1.3 Compared Performance of Sensor Stability.

The stability of immobilized GABAse was tested for its ability to withstand multiple use over time. Sequential measurements were taken for individual fiber sensors. The reproducibility of the response using one sensor is very good. Typically, the activity of the GABAse immobilized on the fibers was approximately 75% of the initial response. However, the response magnitude could vary when a new sensor was used. This made it necessary to calibrate each new optical fiber sensor from a batch of immobilized fibers.

The sensors were then stored at 0^{o} C for the duration of a week. When utilized for similar reactions, the responses of the sensors were 20% of the initial activity. The RSD for each experiment was ± 2 %. Because of the fragility of a single optical fiber sensor, usage and storage caused the experimental collection of data to become relatively difficult. Optimal storage conditions were found to be at 0^{o} C. Although some data showed excellent enzymatic activity after storage at 25^{o} C in dry air, further experiments need to be completed before recommending such treatment.

5.1.4 Sensitivity and Detection Limit of the Fiber Optic Sensor.

Since the response of the enzyme system activity is dependent on the presence of GABA, α-ketoglutarate and $NADP^+$, the GABA signal related to NADPH fluorescence is directly dependent on $NADP^+$ concentration. Figure 5.6 shows the increase in the reaction rate of the enzyme when 100 μM GABA and 100 μM α-ketoglutarate are present in the capillary reactor with increasing $NADP^+$ concentration, from 0 to 1 mM. The sensor was calibrated with an excess $NADP^+$ solution of 1 mM.

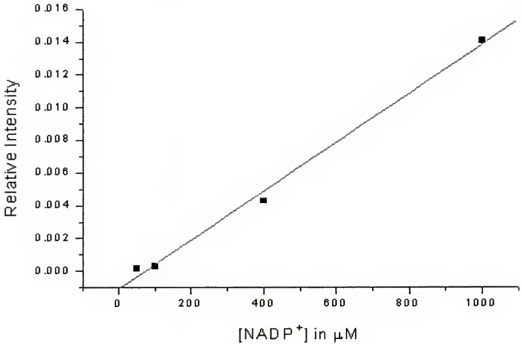

Figure 5.6 Effect of NADP$^+$concentration on the GABA sensor activity.

Figure 5.7 shows the relationship of the enzymatic signal versus α-ketoglutarate concentration. At concentrations over 100 μM α-ketoglutarate, we see that there is no longer an influence on the reaction kinetics detected. The sensor calibration curve was monitored in the presence of excess α-ketoglutarate.

The effect on the sensor of varying the GABA concentration is shown in Figure 5.8. The insert shows the linear relationship of GABA concentration versus the rate of the enzymatic reaction. The relative rate of increase in fluorescence intensity is plotted versus GABA concentration in the 0 to 100 μM range. The standard curve taken from this sensor shows glutamate has a detection limit of 0.92 μM (as shown in Figure 5.9).

This limit of detection is adequate for measurements taken at the physiological level of cellular release (which is typically in the millimolar range). The sensitivity of our probe and optical arrangement for detection has proven an excellent base from which we can build additional biomolecule sensors.

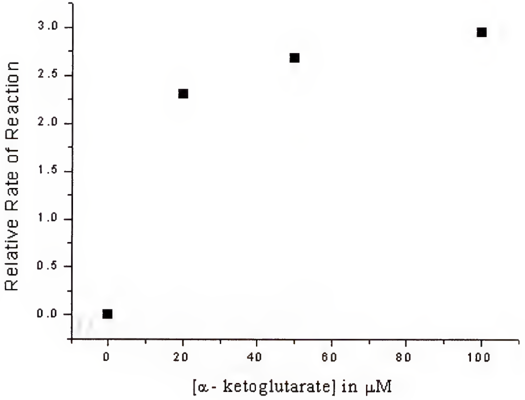

Figure 5.7 Effect of α-KG concentration on the GABA sensor activity.

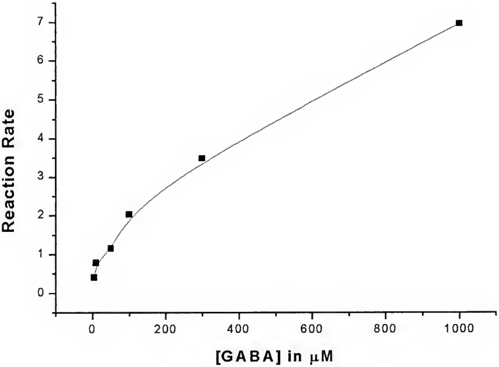

Figure 5.8 GABA calibration plot using a GABAse probe with $NADP^+$ and α-KG at 1 mM.

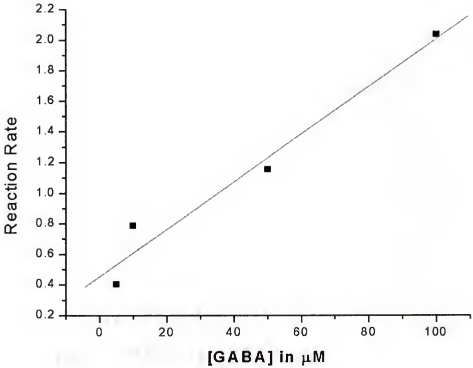

Figure 5.9 Linear range of detection for GABA sensor. $NADP^+$ and α-KG are at 1 mM.

5.2 Conclusions

Ultrasensitive GABA optical sensors have been developed by directly immobilizing the two enzyme system, GABAse, onto optical fiber probe surfaces through newly developed covalent binding mechanisms. Immobilization procedures used in the design of the glutamate sensor were utilized and confirmed to be a widely applicable procedure to coordinate the enzyme molecules to the optical fiber tip. Optimal immobilization of GABAse occurred around 19 hours in the enzyme solution. The GABAse molecules on the optical fiber surface have high enzymatic activity. The sensor's detection concentration limit is 0.93 μM GABA. Our detection system can monitor NADH and NADPH generated by the sensor. The GABA sensor is stable and reliable after storage at 0^{o} C. These probes will be useful to the study subcellular level neurophysiological response in GABA release monitoring experiments.

There are a number of enzyme kinetic studies that could be planned using optical detection methods and the GABAse immobilized at the tip of a fiber. Once the enzyme has been immobilized, certain characteristics of the enzyme's preferred conformation with one another appear in the signal monitored by the production of NADPH. There are many possible reaction mechanisms that may transpire due to availability of individual active sites on each enzyme and thermodynamic or equilibrium effects from concentrations of product. In the future, this biosensor may aide in the understanding of GABAse function and structure in the overall biochemical scheme of these enzymatic reactions.

CHAPTER 6
CURRENT AND FUTURE APPLICATIONS

There are many fatal diseases that disrupt the complex system of neurons in the central nervous system. Understanding of a few, if not all neurotransmitters will greatly increase our knowledge of neurological disease progression and cause. Advances in this field will pave the way for effective treatments and possibly prevention or a cure of diseases like ischemic stroke, epilepsy and Huntington's Chorea. Monitoring levels of glutamate and GABA present in the extracellular fluid of a neuronal synapse will eventually aid in the comprehension of neuronal physiology. With the design of the glutamate and GABA fiber optic biosensor, a numberof experimental possibilities, described below, become available to study these neurological diseases.

6.1 Immobilization Techniques

The novel biosensors developed in this thesis work are highly reactive, even though they are based on a very simple enzyme immobilization method. The testing and combination of several immobilization parameters has led to the basic methodology described in the text. The creation of two biosensors, a GDH fiber optic probe as well as a GABAse (two-enzyme) fiber optic probe, enables the development of a variety of biomolecule probes using enzymes, antibodies, DNA molecules, neurotransmitters and peptides. The immobilization mechanism used for these biosensors enables the detection of biological analytes in a system more similar to free solution, rather than in the confines of gel or protein matrices. Advantages of this method reside in its ability to decrease diffusion limitation, eliminate non-uniform distribution of biomolecules at the sensor surface, and regenerate sensor activity quicker. As surface immobilization technology of biomolecules advances, the creation of more efficient and sensitive fiber optic biosensors will follow.

6.2 Nanofabrication of Probes

The potential of these fiber optic probes has substantially impacted the study of single cells. Using NFO technique, the feasibility of monitoring the mechanisms of stroke at the cellular level and subcellular level have been proven successful in initial trials. The spatially limited study of cell structure and processes has been overcome by nanofabrication of optical fiber probes. Nanometer dimension NFO probes can monitor intracellular events either on the cell's membrane or inside a living cell [39], by virtue of a method devised to introduce a NFO probe into a *live* cultured neuroblastoma or smooth muscle cell.

Microscopic investigations were accomplished with miniaturization of the probe size by means of pulling and/or etching optical fiber probes. Optical fiber probes from 100 nm to tens of micrometers were prepared. Etched tips have been confirmed to have higher light throughputs than pulled tips. This improvement in transmission efficiency is a result of the larger cone angles and shorter tapers of the etched tips. It can be concluded that etched tips are preferred in experiments where higher light throughput is desired. The etching technique has been successfully used in the fabrication of ultrasmall probes that have the capability to detect glutamate in living cells. A probe size in the sub-5 micrometer region has proven to be sufficient for initial glutamate and GABA mapping experiments on the single cell level (Figure 6.1). Upon proper placement of the sensor and stimulation of the cell, neurotransmitter release could be monitored. Future applications of this technique will be used in the creation of various other biosensors, including a GABA sensor. These sensors have the ability to improve the spatial resolution of existing optical sensors by at least a factor of 1000 ($\leq 0.1 \mu m$ vs. 100 μm), the temporal resolution by a similar factor ($\leq$20 ms vs. 10 s), and the sample size by a factor of a billion (femtoliters vs. milliliter) [5]. The present sensors are not only selective and essentially noninvasive, but also flexible and difficult to be broken when touching a surface. The nanofabrication of fiber probes capitilizes on the demonstrated ability to construct such robust and ultra-small sensors.

6.3 Multi-Functional Senors

Cellular level studies must be performed in extremely small volumes or areas. The restricted detection area dictates the size of the probe for use in cellular monitoring. Multifunctional single fiber probe sensors can be created on the basis of the two-enzyme GABA sensor. There are several cellular level studies that would be advanced by the development of dual sensors. These sensors could be enhanced by either combining stimulation and measurement, or simultaneously detecting several intracellular species, such as glutamate and lactate.

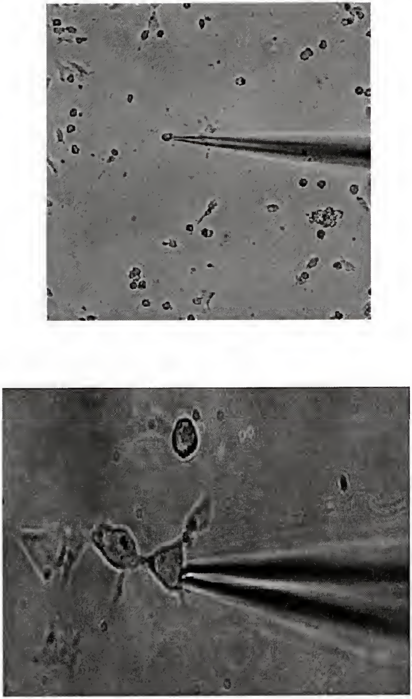

Figure 6.1 CCD image of preliminary cellular applications of a micrometer sized glutamate fiber sensor.

To study the cell at more than just one point and for more than just one analyte, these nanometer-sized tips have also been used in the nanofabrication of arrayed structures [42], generating possible applications in the development of arrayed biosensors. Biosensor arrays are intended for imaging and sensing *in vivo* biological processes with superior analyte sensitivity and specificity. They are capable of obtaining simultaneous biochemical measurements at multiple points on a subcellular level. The development of arrayed biosensors is of great interest and will be applied in studies of multiple cellular events or for monitoring of numerous cells simultaneously. For example, ischemic cell death occurs when extracellular glutamate levels increase, causing tissue depolarization and an excessive rise in intracellular [Ca^{2+}]. Two adjacent cells could be monitored to study the spread of cell damage. As shown in Figure 6.2, the two sensors will be placed in different areas: a glutamate sensor between cell 1 and 2, and a Ca^{2+} sensor [1] inside cell 2. Only neuron 1 receives an insult resulting in ischemic cell death. Once cell 1 has been stimulated (e.g. hypoxia or the drug, NMDA), simultaneous determination of Ca^{2+} and glutamate would be carried out. Fabrication of arrayed biosensors can produce real-time biochemical imaging and sensing of subcellular processes in living cells. Biosensor arrays are advantageous because they allow for multiple detection at different sites and of different species with high resolution at each point measurement.

6.4 Optical Set-Up

Fiber optic enzyme sensors involve state of the art optical detection mechanisms. The SPCM-200 model APD, used in this research, is a self contained module which detects photons of light over the wavelength range of 400 nm to 1060 nm; range and sensitivity which often out performs photomultiplier tubes. Although this APD is sensitive (50-55% photon detection efficiency), newer models have surpassed these limits. EG&G's most advanced APD, the SPCM-151, can monitor a maximum of five million counts per second. This model has 70% photon detection efficiency in addition to a much lower dark count. Our optical detection set-up has the potential to be upgraded for higher sensitivity to detect even smaller fluorescence signals from anticipated subcellular applications. By enhancing the detection system, many new experimental protocols become available.

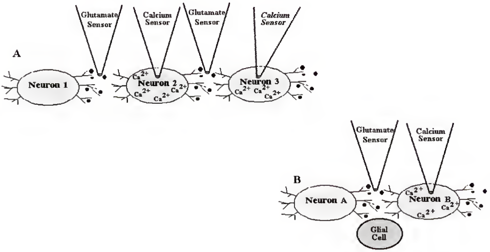

Figure 6.2 Schematic drawing of simultaneous determination of extracellular glutamate and intracellular calcium in ischemic neuronal damage.

6.5 Synopsis

The capability now exists to apply these physical techniques to the research of biological structures and functions. The results documented herein will influence the development of techniques that measure optical properties of living samples with a level of resolution previously not available in any field of science. We anticipate that the methodologies developed in our labs will be widely used in biomedical research, providing new opportunities to monitor biological events at the single cell, and even single molecule level. Future biological research now has the potential to surpass the constraints of conventional science by using the NFO capabilities of optical fiber biosensors.

LIST OF REFERENCES

1. Tan, W. Ph. D. Thesis: University of Michigan, **1993**.

2. Resnick, R.; Halliday, D.; Krane, K. *Physics; Fourth Edition*, John Wiley &Sons: New York, 1992.

3. Betzig, E.; Trautman, J. K.; Harris, T. D.; Weiner, J. S.; Kostelak, R. L. *Science* **1991**, *251*, 1468-1470.

4. Munkholm, C.; Walt, D. R.; Milanovich, F. P.; Klainer, S. M. *Anal. Chem.* **1986**, *58*, 1427-1430.

5. Tan, W.; Shi, Z. Y.; Smith, S.; Birnbaum, D.; Kopelman, R. *Science* **1992**, *258*, 778-781; Tan, W.; Shi, Z. Y.; Kopelman, R. *Anal. Chem.* **1992**, *64*, 2985-2990.

6. Rosenzweig, Z.; Kopelman, R. *Anal. Chem.* **1995**, *67*, 2650-2654; Rosenzweig, Z.; Kopelman, R. *Anal. Chem.* **1996**, *68*, 1408-1413.

7. Hu, Y.; Mitchell, K. M.; Albahadily, F. N.; Michaelis, E. K.; Wilson, G. S. *Brain Research* **1994**, *659*, 117-125; Hu, Y.; Wilson, G. S. *J. Neurochem.* **1997,** *69*, 1484-1490.

8. Garguilo, M. G.; Michael, A. C. *J. Neurosci. Methods* **1996**, *70,* 73-82.

9. Pantano, P.; Walt, D. R. *Anal. Chem.* **1995**, *67,* 481A-487A.

10. Liu, B.; Hu, R.; Deng, J. *Anal. Chem.* **1997**, *69*, 2343-2348.

11. Chrisey, L. A.; Lee, G. U.; O'Ferrall, C. E. *Nucl. Acid. Res.* **1996**, *24*, 3031-3039.

12. Bickerstaff, G. F. *Immobilization of Enzymes and Cells*; Humana Press Inc.: New Jersey, 1997; pp 331-337.

13. Piunno, P. A. E.; Ulrich, J. K. *Anal. Chem.* **1995**, *67*, 2635-2643.

14. Herdan, J. M.; Balulescu, M.; Cira, O. *J. Mol. Catalysis* **1996**, *107*, 409-414.

15. Weetall, H. H. *Appl. Biochem. Biotechnol.* **1992**, *33*, 139-143.

16. Bang, L. Undergraduate Thesis: University of Florida, **1998**.

17. Manyam, N. V.; Hare, T. A.; Katz, L. *Life Sci.* **1980**, *26*, 1303-1308.

18. Pantano P.; Kuhr, W. G. *Anal. Chem.* **1993**, *65,* 623-630.

19. Bunin, M. A.; Wightman R. *J.Neurosci.* **1998,** *18,* 4854-4860.

20. Ingersoll, C. M.; Bright, F. V. *Anal. Chem.* **1997**, *69*, 403A-408A.

21. Wang, A. J.; Arnold, M. A. *Anal. Chem.* **1992**, *64*, 1051-1055; Kar, S.; Arnold, M. A. *Anal. Chem.* **1992**, *64*, 2438-2443.

22. Dremel, B. A.; Schmid, R. D.; Wolfbeiss, O. S. *Anal. Chim. Acta* **1991**, *248*, 351-359.

23. Lada, M. W.; Vickroy, T. W.; Kennedy, R. T. *Anal. Chem.* **1997**, *69*, 4560-4565.

24. Wang, Z.; Yeung, E. S. *J. Chromatogr. B. Biomed. Sci. Appl.* **1997**, *695*, 59-65.

25. Niwa, O.; Torimitsu, K.; Morita, M.; Osborne, P.; Yamamoto, K. *Anal. Chem.* **1996,** *68,* 1865-1870.

26. Chen, G.; Ewing, A. G. *Crit. Rev. Neurobiol.* **1997**, *11*, 59-90.

27. Korenbrot, J.; Perry, R.; Copenhagen, D. R. *Anal. Biochem.* **1987**, *161*, 187-199.

28. Niwa, O.; Kurita, R.; Tsutomu, H.; Torimitsu, K. *Anal. Chem.* **1998**, *70*, 89-93.

29. Boyd, B.; Kennedy, R. T. *The Analyst*, in press.

30. Sethi, M. L. *J. Pharm. Biomed. Anal.* **1993**, *11,* 613-617.

31. Qu, Y.; Arckens, L.; Vandenbussche, E.; Geeraerts, S.; Vandesande, F. *J. Chrom.* **1998**, *798*, 19-26.

32. Israel, M.; Lesbats, B. *J. Neurochem.* **1996**, *67,* 2624-2627.

33. Subramanian, S. *Biophys. Chem.* **1978**, *7*, 375-378.

34. Zivin, J. A.; Choi, D. W. *Scien. Amer.* **1991**, *265*, 56-63.

35. Scott, E.; Jakoby, W. B. *J. Biol. Chem.* **1959**, *234*, 932-936.

36. Rosenzweig, Z.; Kopelman, R. *Anal. Chem.* **1997**, *67*, 2650-2654; Barker, S. L. R.; Kopelman, R.; Meyer, T. E.; Cusanovich, M. A. *Anal. Chem.* **1998**, *70*, 971-976.

37. Shortreed, M. R.; Bakker, E.; Kopelman, R. *Anal. Chem.* **1996**, *68*, 2656.

38. Uttamchandani, D.; McCulloch, S. *Adv. Drug Deliv. Rev.* **1996**, *21*, 239.

39. Tan, W.; Bang, L.; Cordek, J.; Liu, X. *SPIE-Int. Soc. Opt. Eng.* **1998**, *3273*, 186-192.

40. Sogowa, K.; Takahashi, K. *J. Biochem. (Tokyo),* **1978**, *83*, 1783.

41. Tan, W.; Yeung, E. *Anal. Chem.* **1997**, *69*, 4242.

42. Michael, K. L.; Taylor, L. C.; Schultz, S. L.; Walt, D. R. *Anal. Chem.* **1998**, *70*, 1242-1248; Healey, B. G.; Li, L.; Walt, D. R. *Biosens. Bioelectron.* **1997**, *12*, 521-529.

BIOGRAPHICAL SKETCH

Julia M. Cordek was born in Winter Park, Florida in 1972. She graduated from Lyman High School in Longwood, Florida in 1990. In August 1990, she entered Stetson University and received the degree of Bachelor of Science in chemistry, with a minor in German, in May 1994. She then became an environmental health specialist for NASA at Kennedy Space Center, Florida, where she worked for two years. She entered graduate school in chemistry at the University of Florida in August 1996 and received the degree of Master of Science in December 1998.

I certify that I have read this study and that in my opinion it conforms to acceptable standards of scholarly presentation and is fully adequate, in scope and quality, as a thesis for the degree of Master of Science.

Weihong Tan, Chair
Assistant Professor of Chemistry

I certify that I have read this study and that in my opinion it conforms to acceptable standards of scholarly presentation and is fully adequate, in scope and quality, as a thesis for the degree of Master of Science.

James Winefordner

James D. Winefordner
Graduate Research Professor of Chemistry

I certify that I have read this study and that in my opinion it conforms to acceptable standards of scholarly presentation and is fully adequate, in scope and quality, as a thesis for the degree of Master of Science.

C Batich

Christopher D. Batich
Professor of Materials Science and Engineering

This thesis was submitted to the Graduate Faculty of the Department of Chemistry in the College of Liberal Arts and Sciences and to the Graduate School and was accepted as partial fulfillment of the requirements for the degree of Master of Science.

December 1998

Dean, Graduate School